Poisson's Ratio Characteristic Curve of Unsaturated Soils

Sannith Kumar Thota, S.M.ASCE[1]; Toan Duc Cao, A.M.ASCE[2]; and Farshid Vahedifard, M.ASCE[3]

Abstract: Poisson's ratio is an elastic property needed as input in a wide range of geotechnical engineering applications. Despite experimental evidence, there is currently no model in the literature to explicitly account for the effect of saturation on the Poisson's ratio. This paper presents the concept of Poisson's ratio characteristic curve (PRCC), which establishes a relationship between Poisson's ratio and degree of saturation (or matric suction). The PRCC concept is developed based upon the observation that variations of Poisson's ratio are mainly dominated by water retention mechanisms. A sigmoidal function is employed to describe the PRCC with two fitting parameters, funicular degree of saturation and pore fluid continuity, and both are related to the soil water retention curve (SWRC). The functional form is calibrated and validated against Poisson's ratios calculated from measured compressive and shear wave velocities from experimental data sets for 22 different soils from the literature. Further, a set of laboratory tests is performed to measure wave velocities using bender elements and determine the Poisson's ratio of Bonny silt at different suctions. The PRCC fitting parameters are shown to be linearly correlated with the SWRC fitting parameters. To illustrate the PRCC application, three sets of laboratory-measured data of at-rest earth pressure coefficient for different unsaturated soils are collected from the literature and compared against the predicted values using the PRCC model and those using constant Poisson's ratio values. The values using the PRCC model closely match the measured values, whereas using a constant Poisson's ratio can significantly underpredict or overpredict the at-rest earth pressure coefficient. The proposed model can readily be incorporated into analytical and numerical models, leading to more accurate assessments of unsaturated soil behavior. **DOI: 10.1061/(ASCE)GT.1943-5606.0002424.** *© 2020 American Society of Civil Engineers.*

Author keywords: Unsaturated soil; Poisson's ratio; Degree of saturation; Poisson's ratio characteristic curve; Soil water retention curve.

Introduction and Background

Poisson's ratio is an elastic property of soil defined as the ratio of lateral strain to longitudinal strain under uniaxial loading (e.g., Salem 2000; Fredlund et al. 2012). The property can vary between 0 and 0.5 for soils depending on various factors such as soil type, density, confining pressure, porosity, and degree of saturation among others (e.g., Salem 2000; Velea et al. 2000; Inci et al. 2003; Gao et al. 2013; Suwal and Kuwano 2013). Poisson's ratio is close to zero when there is no lateral movement as the soil is loaded in a uniaxial direction. It reaches 0.5 when there is no volumetric change in the soil specimen. Typically, the range of Poisson's ratio for stiff to soft clays is 0.20–0.45, for silts is 0.20–0.35, and for dense to loose sands is 0.15–0.35 (Budhu 2010; Fredlund et al. 2012). Poisson's ratio is needed as input in a wide range of analytical analyses and numerical simulations (e.g., finite element) for saturated and unsaturated soils including slope stability, earth pressure, settlement, bearing capacity, and swelling and shrinkage (e.g., Lu and Likos 2004; Fredlund et al. 2012; Oh and Vanapalli 2018). For unsaturated soils, the dependency of Poisson's ratio on water content or degree of saturation is widely demonstrated through several experimental studies reported in the literature (e.g., Inci et al. 2003; Gao et al. 2013; Shin et al. 2016; Patel et al. 2018). The same observation is reported by back calculating Poisson's ratio using the relationship between Young's and shear moduli (e.g., Oh and Vanapalli 2011, 2016).

Poisson's ratio of unsaturated and saturated soils can also be experimentally determined through measurements of shear and compressional wave velocities. Several laboratory testing methods have successfully been used to measure shear and compressional wave velocities in different soils using techniques such as the bender elements method, ultrasonic testing devices, and piezoelectric transducers (e.g., Velea et al. 2000; Inci et al. 2003; Valle-Molina 2006; Byun et al. 2013; Irfan and Uchimura 2013; Taylor et al. 2019). Various field tests such as seismic reflection and refraction, seismic cross-hole and down-hole, and seismic cone penetration can also be used to measure velocities to determine the Poisson's ratio of soils (e.g., Luna and Jadi 2000; Ayres and Theilen 1999; Cosentini and Foti 2014). These dynamic tests provide P- and S-wave velocity measurements within the small strain linear elastic range. Thus, understanding the small strain behavior of soils is important for several applications including predicting ground movements, studying soil liquefaction, and assessing the performance of engineering structures (e.g., tunnels, retaining walls, and pipeline) and slopes under working conditions (e.g., Clayton 2011; Likitlersuang et al. 2013; Yang and Gu 2013; Dong et al. 2016).

All the aforementioned experimental studies report that the shear and compressive wave velocities vary, and Poisson's ratio increases with an increase in the degree of saturation of the soil.

[1]Ph.D. Student, Dept. of Civil and Environmental Engineering, Mississippi State Univ., Mississippi State, MS 39762. Email: st1545@msstate.edu

[2]Postdoctoral Research Associate, Center for Advanced Vehicular Systems (CAVS) and Dept. of Civil and Environmental Engineering, Mississippi State Univ., Mississippi State, MS 39762. Email: toand@cavs.msstate.edu

[3]Civil and Environmental Engineering Advisory Board Endowed Professor and Associate Professor, Dept. of Civil and Environmental Engineering, Mississippi State Univ., Mississippi State, MS 39762 (corresponding author). ORCID: https://orcid.org/0000-0001-8883-4533. Email: farshid@cee.msstate.edu

Note. This manuscript was submitted on October 20, 2019; approved on August 10, 2020; published online on October 22, 2020. Discussion period open until March 22, 2021; separate discussions must be submitted for individual papers. This paper is part of the ***Journal of Geotechnical and Geoenvironmental Engineering***, © ASCE, ISSN 1090-0241.

However, there is currently no model for Poisson's ratio in the literature to explicitly account for the effect of the degree of saturation (Oh and Vanapalli 2018). Because of this gap, all analyses, even complex numerical simulations, of unsaturated soils have used a constant Poisson's ratio, an assumption that can pose errors in analyses depending on the soil type and degree of saturation. It can be both theoretically and practically beneficial to have a model that can reasonably estimate Poisson's ratio for different unsaturated soil types. To address this need, this paper for the first time presents the concept of Poisson's ratio characteristic curve (PRCC), which establishes a relationship between Poisson's ratio and the degree of saturation (or matric suction) in unsaturated soils. The proposed model is calibrated and validated against Poisson's ratios calculated from measured compressive and shear wave velocities from experimental data sets for 22 different soils from the literature. Further, a set of laboratory tests is performed to measure wave velocities using bender elements and determine Poisson's ratio of Bonny silt at different suctions. Application of the PRCC is demonstrated by comparing the predicted at-rest earth pressure coefficients using the PRCC model, those using constant Poisson's ratio values, and three sets of laboratory-measured data.

Conceptual Model for Poisson's Ratio Characteristic Curve

In this study, the PRCC concept is developed based upon the observation that variations of Poisson's ratio in unsaturated soils are mainly dominated by water retention mechanisms. This observation is supported by the experimental test results reported in the literature (e.g., Inci et al. 2003; Shin et al. 2016; Gao et al. 2013). Fig. 1(a) illustrates the definition of Poisson's ratio as a measure of contraction or extension resulting from the application of longitudinal load under compression or tension. Fig. 1(b) schematically depicts the soil water retention curve (SWRC) (solid black line) and PRCC (solid blue line), defining the variations in matric suction and Poisson's ratio with the degree of saturation, respectively. Both curves exhibit a similar sigmoidal shape. It is well known that several properties of unsaturated soils (e.g., strength, stiffness) are linked to or dominated by water retention mechanisms. As shown by previous studies (e.g., Lu and Dong 2015; Başer et al. 2016), different water retention regimes can be characterized using a sigmoidal shape. Therefore, such a sigmoidal function is employed by others including by Lu and Dong (2015) to define thermal conductivity function and by Başer et al. (2016) to define heat capacity function for unsaturated soils. For the same reason, we adopt a similar sigmoidal shape in this study to link the PRCC to different water retention mechanisms.

Building upon the aforementioned concept and by employing a sigmoid function, we propose the following generalized equation for the PRCC of unsaturated soils:

$$\mu = \mu_d + (\mu_s - \mu_d)\left[1 - \left\{1 + \left(\frac{S}{S_{fun}}\right)^{n_1}\right\}^{1/n_1 - 1}\right] \qquad (1)$$

where μ = Poisson's ratio; μ_d and μ_s = Poisson's ratios at the dry and fully saturated states, respectively; S = degree of saturation; S_{fun} = degree of saturation at which the funicular regime is onset; and n_1 = pore-water continuity parameter. The two fitting parameters of S_{fun} and n_1, used in the proposed PRCC are related to fitting parameters of the residual degree of saturation (S_r) and pore size distribution (n) commonly employed in SWRC models (e.g., van Genuchten 1980). Current trends in the state of the art in unsaturated soil mechanics lean more toward employing matric

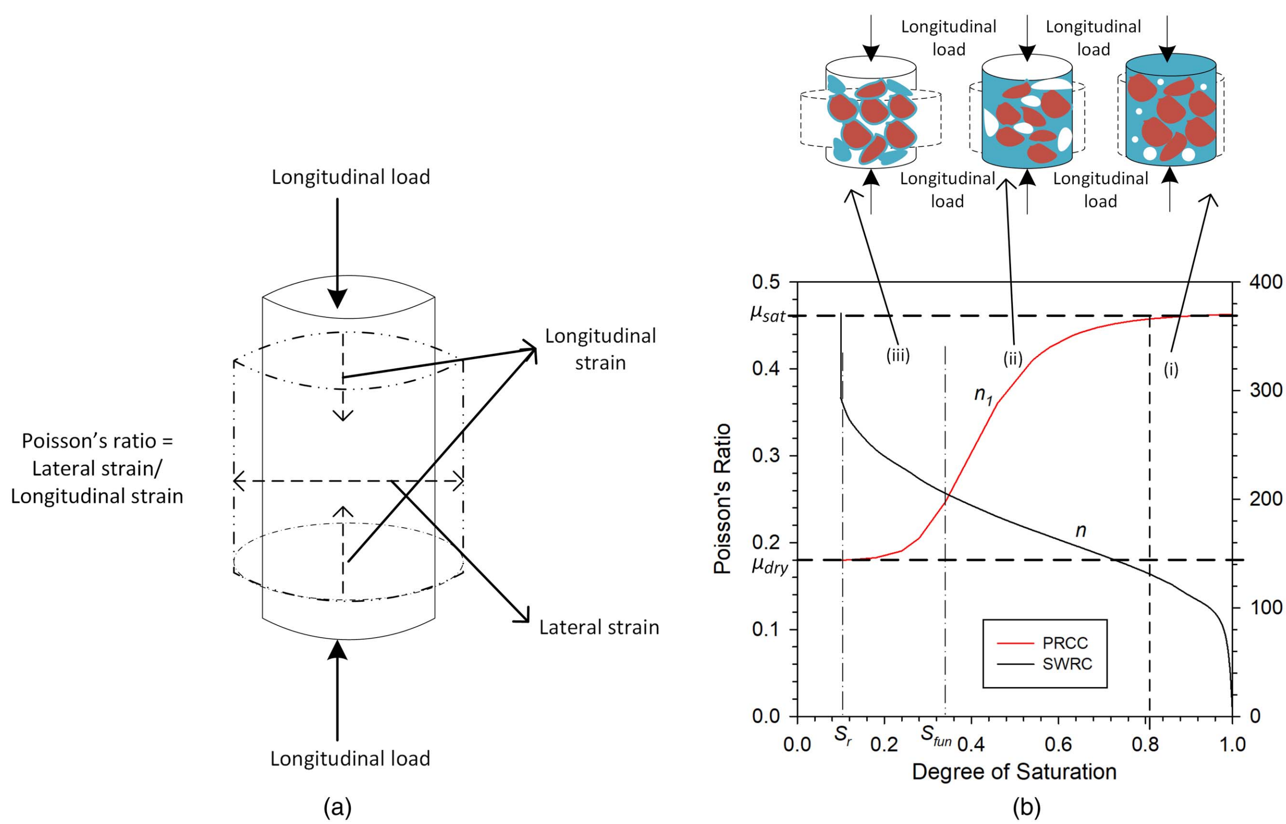

Fig. 1. Poisson's ratio in soils: (a) definition; and (b) Poisson's ratio and matric suction versus degree of saturation.

suction instead of the degree of saturation to be more mechanistic. Thus, Eq. (1) can be rewritten as a function of matric suction using the van Genuchten (1980) SWRC model as follows:

$$\mu = \mu_d + (\mu_s - \mu_d) \times \left[1 - \left\{1 + \left(\frac{(1 + (\alpha(u_a - u_w))^n)^{1/n-1}}{S_{fun}}\right)^{n_1}\right\}^{1/n_1-1}\right] \quad (2)$$

where u_a and u_w = pore-air and pore-water pressures, respectively, and the difference between the two represents the matric suction; and α = fitting parameter related to air-entry suction.

It is noted that the proposed formulation is developed under the assumption of elastic, isotropic, and homogeneous materials.

The SWRC possesses three different stages of desaturation based on capillarity and adsorption mechanisms of the soil. As shown in Fig. 1(b), these stages are generally categorized as (1) capillary, where air phase is in the form of bubbles; (2) funicular or continuous water phase, where menisci are interconnected with each other; and (3) pendular or discontinuous water phase, where the water forms menisci near particles (Lu and Likos 2004, 2006). It is well documented in the literature (e.g., Cho and Santamarina 2001; Lu and Likos 2004; Salager et al. 2007) that the fitting parameters of SWRC models are related to different states of the capillary, funicular, and pendular of the soil drying curve schematically shown in Fig. 1(b). In the capillary state, all the voids are filled with liquid and are held into the pores under capillary action with some air bubbles in the system. In the funicular state, where the voids are not fully saturated with liquid, the water still forms a continuous phase. The rate of change in the degree of saturation is high in this state up to the funicular degree of saturation (S_{fun}), representing a transition between the funicular and pendular states. The pendular state begins either when water and air become discontinuous or the air becomes continuous, and water films form around particles when the adsorption phenomenon is dominant (e.g., Pietsch 1991; Leverson and Lohnes 1995; Cho and Santamarina 2001). In the SWRC models, the capillary and funicular states can be represented through air-entry and pore size distribution fitting parameters. In the drying path, the air-entry parameter determines the transition between saturated and unsaturated state and the pore size distribution parameter determines the rate at which desorption in the soil can occur. The pendular state of the SWRC determines the residual and dry states of the soil. Though fitting parameters, they are successfully linked to the dominating water retention mechanisms and are correlated to soil physical properties such as the soil particle size distribution, soil texture, and bulk density (or void ratio) in several studies (e.g., Gupta and Larson 1979; Saxton et al. 1986; Vereecken et al. 1989; Wang et al. 2017).

Similar to the SWRC, the PRCC has different stages and varies between dry and saturated states, and these can be represented by three water retention regimes [Fig. 1(b)]. Poisson's ratio is a minimum at the dry state because of the relatively higher compressibility of the soil and is a maximum at the saturated state (e.g., Salem 2000; Patel et al. 2018) because the soil is almost incompressible, and no volume change occurs in the soil. In other words, saturated soils are almost incompressible and exhibit higher Poisson's ratio. As the degree of saturation decreases, and the water phase becomes discontinuous, the compressibility of soil increases, and therefore the Poisson's ratio decreases. The laboratory-measured data show that as a soil transitions from saturated to unsaturated state, both the degree of saturation and Poisson's ratio decrease with different rates depending on the dominant water retention state (e.g., Inci et al. 2003; Kumar and Madhusudhan 2012; Suwal and Kuwano 2013; Patel et al. 2018; Dong 2019). The rate of change in Poisson's ratio is minimal in the saturated state (capillary state). It is known that the compressibility of water is negligible compared to the soil matrix. Therefore, at near saturation, the pore water dominates over the soil skeleton; hence, Poisson's ratio is high and almost constant. The saturated Poisson's ratio represents this stage in the proposed PRCC.

As the degree of saturation decreases, the mobilization of deformation in the soil matrix overcomes the pore water dominance, and therefore, the compressibility increases, and in turn, Poisson's ratio decreases. This is the funicular region at which the rate of deformation is high since water menisci are interconnected. In the proposed model, the onset of this region is defined with the funicular degree of saturation before which the rate of change in Poisson's ratio with the degree of saturation is high and after which the rate of change in Poisson's ratio with the degree of saturation is negligibly small. In the funicular region, any local change in matric suction is rapidly redistributed throughout the soil pores by diffusion within the continuous water phase. The drying rate, and subsequently the rate of change in Poisson's ratio is steep in this region represented by the pore-water continuity parameter. In the pendular region, the meniscus is disconnected, and air voids are connected to each other. The matric suction redistribution throughout the soil pores takes place through vapor diffusion, which is a very slow process. The drying rate in this stage is very small; hence, the change in Poisson's ratio with the degree of saturation is negligible. This region is represented by the dry Poisson's ratio in the proposed PRCC formulation.

Database of Experimental Test Results

In this study, a database of experimental data sets of 23 different soils (including 22 soils reported in the literature plus one soil experimentally tested in the current study) is created and used for calibrating and validating the proposed PRCC model. Table 1 shows the properties and the original reference for each of the 23 soils included in the database. Soil Nos. 1–22 are the soils collected from the experimental data in the literature, whereas Soil No. 23 is the soil used in the laboratory tests performed in this study. As shown, the database includes different soil types ranging from clay (5 soils) to silt (4 soils) and sand (5 soils), sand-clay mixtures (4 soils), and sand-silt mixtures (5 soils). It is known that soil stiffens dependently on strain. To minimize any inconsistency in the testing methodologies and strain levels employed to generate the results, the compiled database only includes results obtained using wave velocity measurements (V_p and V_s) from dynamic laboratory tests (e.g., bender element tests), representing comparable small strain elastic conditions.

One can use elastic constants and wave velocities relationships to derive an equation for Poisson's ratio in terms of wave velocities. For an elastic, isotropic, and homogeneous material, the elastic constants are given by (e.g., Inci et al. 2003; Kumar and Madhusudhan 2012; Suwal and Kuwano 2013; Patel et al. 2018)

$$G = \rho V_s^2 \quad (3)$$

$$M = \rho V_p^2 \quad (4)$$

$$E = 2G(1 + \mu) \quad (5)$$

$$E = \frac{M(1 + \mu)(1–2\mu)}{(1 - \mu)} \quad (6)$$

where G, M, and E = elastic constants of shear, constrained, and Young's moduli, respectively; and V_s and V_p = shear and

Table 1. Soil properties used for calibration and validation of the proposed model for the PRCC

Soil No.	Soil name and/or classification	μ_s	μ_d	S_{fun}	n_1	n	S_r	α (kPa^{-1})	Reference
1	Clay	0.215	0.160	0.350	3.15	—	—	—	Alramahi et al. (2010)[a]
2	Silt	0.194	0.155	0.050	1.90	—	—	—	Alramahi et al. (2010)[a]
3	Uniform quartz sand	0.310	0.040	0.400	5.00	—	—	—	Conte et al. (2009)[b]
4	Toyoura sand + 15% non-plastic silt	0.365	0.300	0.200	2.00	—	—	—	Suwal and Kuwano (2013)[c]
5	Uniform sand	0.344	0.329	0.270	3.70	—	—	—	Byun et al. (2013)[c]
6	Edosaki sand	0.410	0.272	0.140	1.80	—	—	—	Irfan and Uchimura (2013)[c]
7	Toyoura sand + 5% kaolin clay	0.340	0.230	0.080	1.68	—	—	—	Suwal and Kuwano (2013)[c]
8	Toyoura sand + 15% kaolin clay	0.380	0.200	0.160	2.00	—	—	—	Suwal and Kuwano (2013)[c]
9	Toyoura sand	0.260	0.247	0.180	3.50	—	—	—	Suwal and Kuwano (2013)[c]
10	Quartz silica beach sand, SP	0.468	0.270	0.156	4.30	—	—	—	Taylor et al. (2019)[d]
11	Poorly graded Sand, SP	0.410	0.272	0.140	1.80	—	—	—	Kumar and Madhusudhan (2012)[e]
12	Toyoura sand + 10% non-plastic silt	0.390	0.290	0.050	1.30	—	—	—	Suwal and Kuwano (2013)[c]
13	River silt (67%) + Ottawa sand (33%)	0.300	0.220	0.350	3.50	—	—	—	Alramahi et al. (2007)[e]
14	River silt (50%) + Ottawa sand (50%)	0.190	0.140	0.200	4.00	—	—	—	Alramahi et al. (2007)[e]
15	River silt	0.280	0.150	0.180	3.10	—	—	—	Alramahi et al. (2007)[e]
16	Boulder clay	0.50	0.18	0.200	3.20	—	—	—	Dong (2019)[e]
17	Denver claystone	0.50	0.30	0.300	3.40	—	—	—	Dong (2019)[e]
18	Sanmenxia silt	0.50	0.26	0.700	8.00	—	—	—	Dong (2019)[e]
19	Silty sand, SM	0.466	0.180	0.110	3.00	1.80	0.18	0.05	Byun et al. (2013)[f]
20	Sandy clay, SC	0.470	0.096	0.360	3.30	1.59	0.37	0.08	Inci et al. (2003)[g]
21	Lean clay, CL	0.417	0.030	0.430	2.80	1.30	0.40	0.08	Inci et al. (2003)[g]
22	Low plastic soil + 25% bentonite, CH	0.450	0.203	0.400	3.10	1.70	0.35	0.07	Inci et al. (2003)[g]
23	Bonny silt	0.435	0.05	0.08	3.10	2.24	0.07	0.05	Current study [e]

[a]Used a piezo-crystal bender transducers to measure wave velocities.
[b]Used a modified oedometer setup with a bender elements to measure wave velocities.
[c]Used a modified triaxial setup with piezoelectric disk transducers to measure wave velocities.
[d]Used an ultrasonic near surface inundation testing device with bender elements to measure wave velocities.
[e]Used a modified triaxial setup with a bender and disk elements to measure wave velocities.
[f]Used a modified volumetric pressure plate extractor with bender and piezo disk elements to measure wave velocities.
[g]Used an ultrasonic device with plate element transducers to measure wave velocities.

compressive wave velocities. After substituting Eqs. (3) and (4) into Eqs. (5) and (6), respectively, the equation for Poisson's ratio can be obtained as (e.g., Inci et al. 2003; Kumar and Madhusudhan 2012; Suwal and Kuwano 2013; Patel et al. 2018):

$$\mu = \frac{0.5\left(\frac{V_p}{V_s}\right)^2 - 1}{\left(\frac{V_p}{V_s}\right)^2 - 1} \tag{7}$$

Experimental Data from Literature

Fig. 2 depicts the measured Poisson's ratio versus the degree of saturation for 18 soils (Soil Nos. 1–18 in Table 1) out of the 23 soils. The data for the remaining five soils (Soil Nos. 19–23) are presented and discussed later and include the soils that the SWRC parameters were readily available through the original reference or the current study. For each soil, at a given degree of saturation, Eq. (7) is used to determine the measured Poisson's ratio (shown by circles in Fig. 2) employing the shear and compressive wave velocities data.

Besides the magnitude of change, the Poisson's ratio for all soils increases with an increasing degree of saturation with the maximum and minimum values seen at the saturated and dry states, respectively. Overall, for different soils, Poisson's ratio varies between approximately 0.10–0.45 from dry to saturated states, respectively. The dependency of the wave velocities' ratio (V_p/V_s), and subsequently Poisson's ratio, on the degree of saturation in soils can be explained as follows. As the soil approaches saturation, the time taken for P- and S- waves to travel from the input end to the receiver end varies. That is, as the degree of saturation varies, the waves have to propagate through both interparticle contacts and water phase; hence, the P- and S- wave velocities vary with the degree of saturation. Experimental test results (e.g., Ishihara et al. 1998; Tamura et al. 2002; Irfan and Uchimura 2013; Gao et al. 2013; Shin et al. 2016) consistently show that V_s decreases as the degree saturation increases. However, contradictory trends are reported for V_p versus the degree saturation in the literature. V_p has been historically used for saturation check in the soil laboratory testing based on the assumption that the Skempton B-value and V_p decrease with decreases in saturation. This assumption has been supported by several experimental studies (e.g., Ishihara et al. 1998; Tamura et al. 2002; Tsukamoto et al. 2002; Leong and Cheng 2016; Taylor et al. 2019). However, there is a second group of studies that clearly show an opposite trend using laboratory-measured data, in which V_p increases with a decrease in water content or degree of saturation (or increase in suction) (e.g., Flammer et al. 2001; Inci et al. 2003; Alramahi et al. 2007; Adamo et al. 2010; Irfan and Uchimura 2013; Gao et al. 2013; Shin et al. 2016). The contradictory trends in the results reported by different references are interesting and warrant further investigation but fall beyond the scope of the current study. These contradictory trends can be possibly due to the effects of confining pressure, initial conditions, hydraulic conductivity, and soil type, among others. Despite the contradictory trends for changes in V_p versus the degree of saturation, the reported results in the literature consistently suggest an increase in (V_p/V_s) with an increase in the degree of saturation. This observation, combined with Eq. (7), implies that increases in the degree of saturation cause an increase in Poisson's ratio. In the derivation [Eq. (7)], the variation of Poisson's ratio with the degree of saturation primarily depends on the ratio of V_p/V_s rather than the single V_p value. Thus, even considering the contradictory results reported for V_p versus the degree of saturation, the results for the calculated Poisson's ratio values are unaffected as the

J. Geotech. Geoenviron. Eng., 2021, 147(1): 04020149

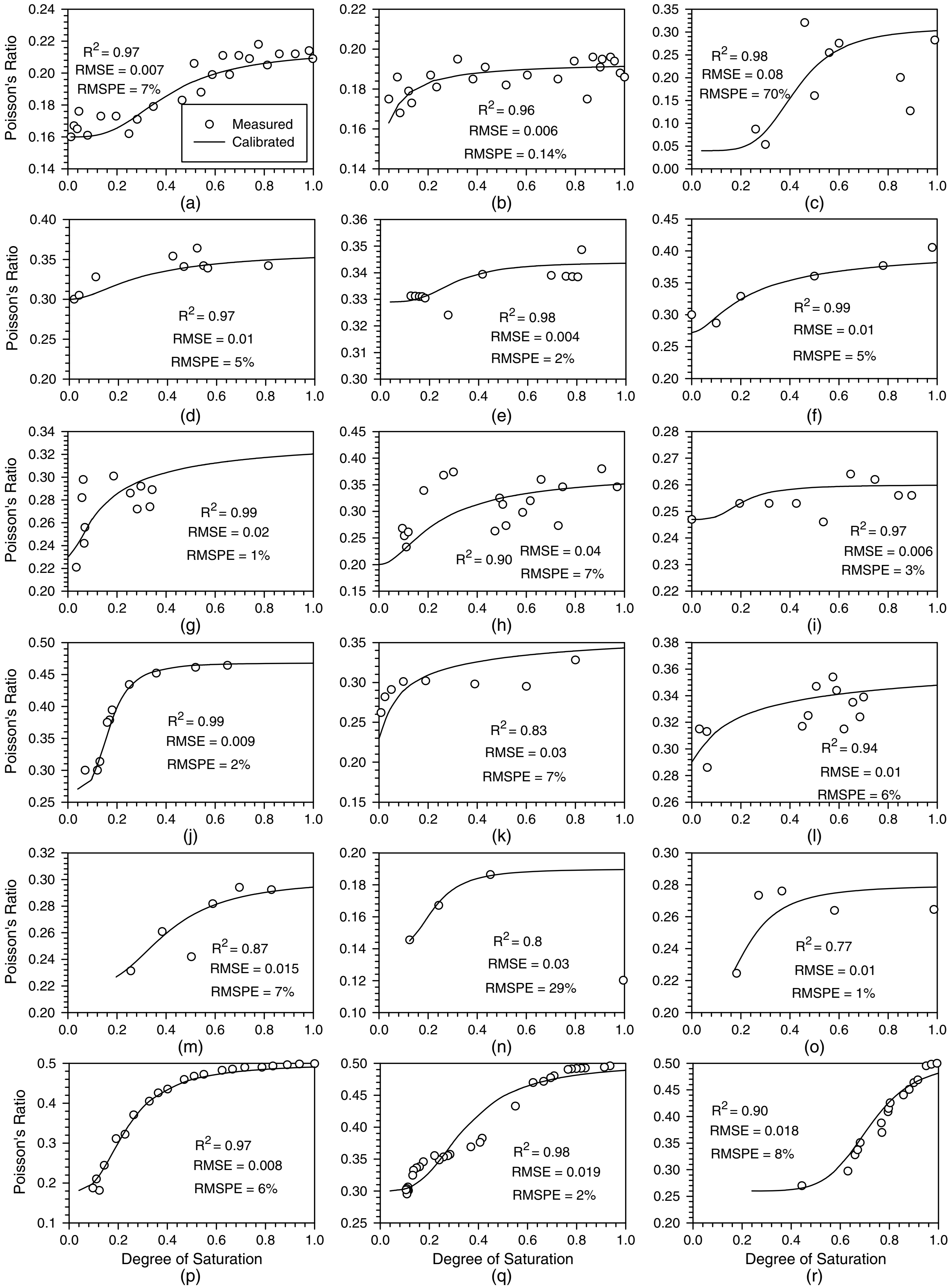

Fig. 2. Measured and calibrated Poisson's ratio with the degree of saturation for Soil Nos. 1–18.

calculation does not involve any assumption (whether increasing or decreasing) regarding the trend for V_p versus the degree of saturation.

It is noted that some soils (e.g., Soil Nos. 3, 7, 8, 12, and 15), visually compared to the others, exhibited more scatter in the measured data. The scatter of data points can be possibly attributed to several factors including the complex characteristics and heterogeneity of pores and the limitations in the testing method. Nevertheless, given the complex nature of the soil behavior, the overall trend follows the proposed sigmoidal shape reasonably well. The variation of the Poisson's ratio with water content is different for fine-grained versus coarse-grained soils. This can be attributed to differences in governing water retention mechanisms and the associated changes in effective stress and elastic volumetric strain due to desaturation in fine-grained versus coarse-grained soils (e.g., Oh and Vanapalli 2018).

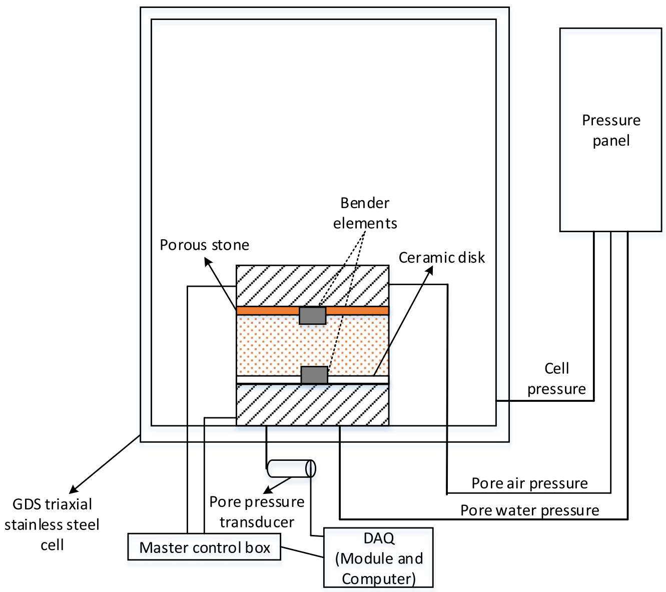

Fig. 3. Line diagram showing the experimental setup used in the laboratory tests.

Laboratory Testing

A set of laboratory tests are performed to measure the shear and compressive wave velocities of Bonny silt (Soil No. 23 in Table 1) at different matric suctions. The tested soil has a liquid limit of LI = 25%, plastic limit of PL = 21%, and specific gravity of $G_s = 2.65$. A modified Bishop-Wesley's triaxial apparatus with bender elements is set up to measure wave velocities at a given matric suction. Fig. 3 shows the line diagram of the complete test setup used in the testing program. Two main systems of pressure panel and bender element method (BEM) are employed in the test setup. A pressure panel allows the user to control confining, air, and water pressures on the specimen; therefore, it can be used to apply matric suction by the axis translation technique. A pair of bender elements are embedded to the top and bottom caps inserted into both sides of the specimen to send and receive wave signals and hence measure wave velocities. Depending on the selection of shear and compressive wave velocity option in the GDS Bender Element version 153 software, the pair of benders elements act as either senders or receivers.

The specimens used in the tests are prepared with a thickness of 25 mm and a diameter of 76 mm. The specimen is compacted under a water content of 10.5% (dry side of optimum) with a void ratio of 0.68 and a maximum dry unit weight of 16.3 kN/m^3. The compacted specimen is placed in the cell and saturation is achieved by reaching a minimum B-value of 0.95. After reaching saturation, the air pressure on the top of the specimen is maintained constant and the water pressure at the bottom is reduced to apply different matric suction in the specimen. The matric suction is applied in intervals from 0 to 240 kPa.

Figs. 4(a and b) depict the measured shear and compressive wave velocities versus the degree of saturation and matric suction, respectively. As shown in Fig. 4(b), both the shear and compressive wave velocities increase with increased matric suction. The V_p/V_s ratio decreases from 2.9 to 1.5 by increasing the matric suction (or decreasing the degree of saturation) from 0 to 240 kPa. The trend of the measured wave velocities ratio supports the observation used to develop the PRCC concept in which the wave velocities ratio (and consequently Poisson's ratio) increases as the degree of saturation increases. Further, the measured water content at each

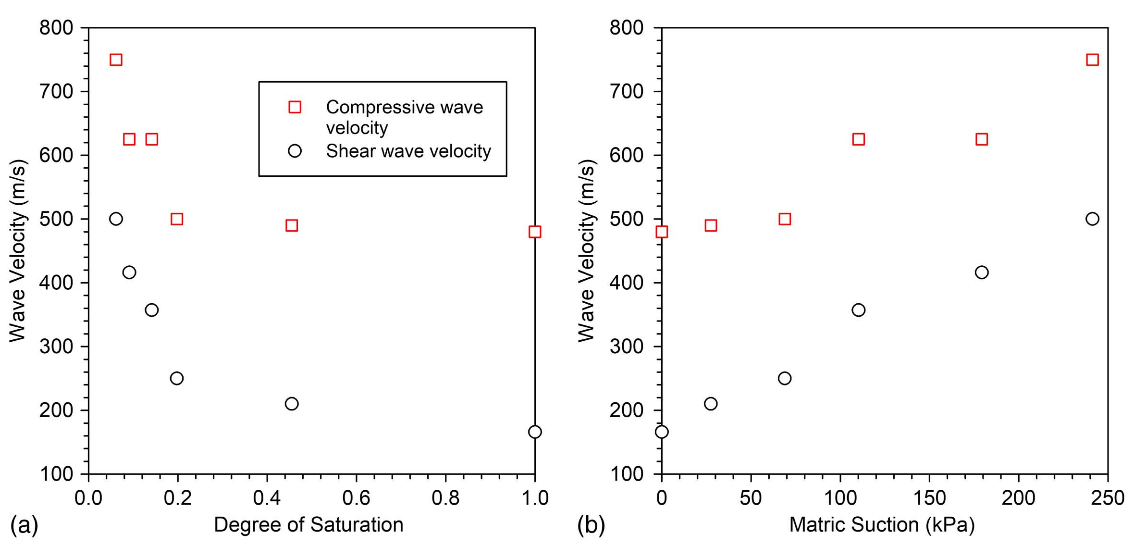

Fig. 4. Measured shear and compressive wave velocities for Bonny silt with (a) degree of saturation; and (b) matric suction.

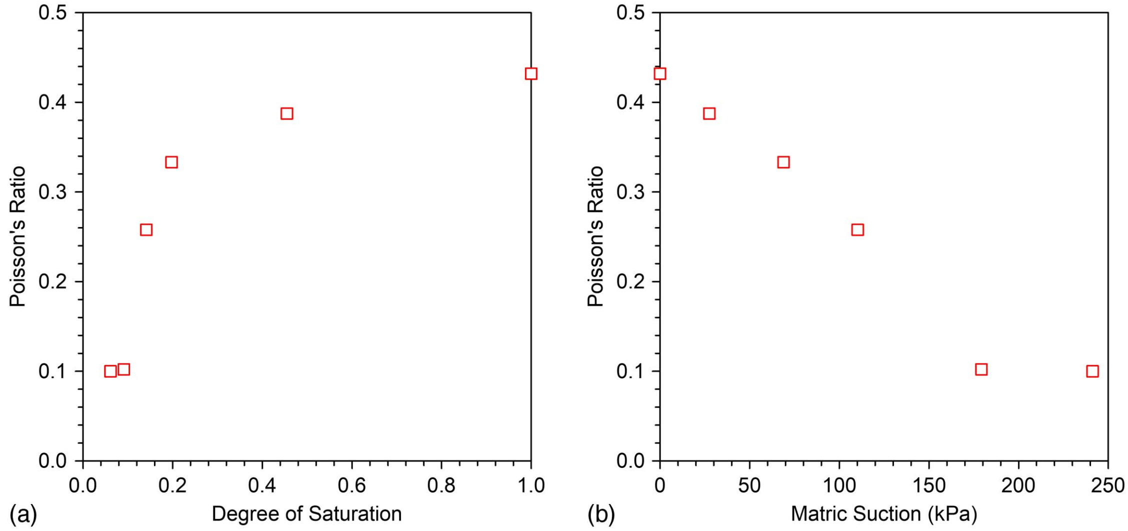

Fig. 5. Measured Poisson's ratio of Bonny silt versus (a) degree of saturation; and (b) matric suction.

matric suction is used to determine the fitting parameters of the van Genuchten (1980) SWRC model for the tested silt (Table 1). Figs. 5(a and b) show the measured Poisson's ratio versus the degree of saturation and matric suction, respectively. The measured Poisson's ratio values are obtained using the measured wave velocities and Eq. (7). The measured data indicate that Poisson's ratio is affected by changes in the degree of saturation (or matric suction), and the relationship follows a sigmoidal shape.

PRCC Model Calibration

For each of the 23 soils, the measured Poisson's ratio values were used along with the least-squares optimization technique to obtain the four parameters (μ_s, μ_d, S_{fun}, and n_1) needed for the PRCC of that soil. The PRCC curve for each soil is drawn using Eq. (1) along with the fitting parameters obtained for that soil. Fig. 2 shows the PRCC curves for Soil Nos. 1–18. Table 1 presents the calibrated parameters for all soils, and Table 2 provides a summary of statistics for the calibrated parameters. The saturated Poisson's ratio varies approximately between 0.2 and 0.5, the dry Poisson's ratio varies between 0.01 and 0.3, the funicular degree of saturation varies between 0.05 and 0.7, and the pore connectivity parameter varies between 1.1 and 8.0.

Analogous to differences in the SWRC variation in fine-grained soils versus coarse-grained soils, the Poisson's ratio of fine-grained soils generally exhibits higher variation with the degree of saturation than coarse-grained soils. This observation has been confirmed by several laboratory studies (e.g., Kumar and Madhusudhan 2012; Suwal and Kuwano 2013; Patel et al. 2018). However, if the soil tested in the laboratory is affected by some external factors or altered, the statement may not hold true anymore. Such factors may change the pore characteristics surrounding solid particles and subsequently can affect the compressibility characteristics and Poisson's ratio behavior of the soil. As considered in the development of the PRCC, the characteristic behaviors of Poisson's ratio for coarse and fine-grained soils consistently follow that for the SWRC of these soils. That is, the SWRC of fine-grained soils generally covers a much wider range of matric suction to transition the soil from saturated to dry states because of the characteristics of pores, notable contribution of adsorbed water, and presence of interparticle forces in these soils.

Using the proposed PRCC model [Eq. (1)] and the calibrated input parameters listed in Table 1, the PRCC curve for each soil is drawn and shown in Fig. 2 for Soil Nos. 1–18. The results for all soils show, in general, good agreement between the calibrated and the measured data. For each soil, three statistical parameters are determined to statistically examine the predictive capability of the proposed model: coefficient of determination (R^2), root mean square error (RMSE), and root mean square percentage error (RMSPE). As shown in Fig. 2, R^2 values are equal or greater than

Table 2. Summary statistics of the calibrated parameters for the Poisson's ratio characteristic curve

Description	μ_s	μ_d	S_{fun}	n_1
Minimum	0.194	0.010	0.05	1.30
Maximum	0.500	0.329	0.70	8.00
Average	0.386	0.187	0.30	3.73
Standard deviation	0.081	0.087	0.16	2.72

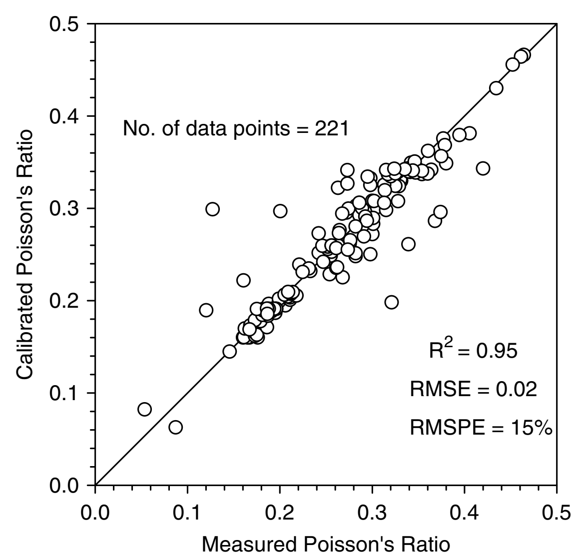

Fig. 6. Comparison of measured and calibrated Poisson's ratio for 18 different soils (Soil Nos. 1–18).

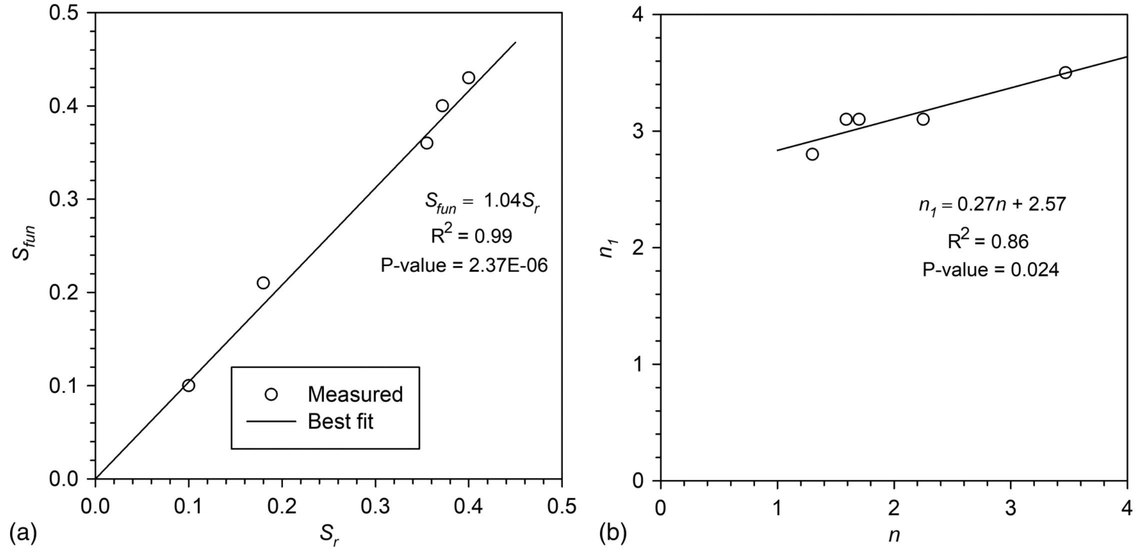

Fig. 7. Correlation between the fitting parameters of the proposed PRCC model and the van Genuchten (1980) SWRC model for Soil Nos. 19–23: (a) S_{fun} versus S_r; and (b) n_1 versus n.

0.9 for all soils (except Soil No. 15 with $R^2 = 0.77$). Further, the RMSE and RMSPE values, which provide the statistical measures of how spread out the prediction errors are, calculated for each soil are low and within the acceptable range for all soils. For the majority of soils, the RMSE is less than 0.05 and the RMSPE is less than 5%, supporting the predictive capability of the PRCC model. A possible reason for relatively high RMSE and RMSPE values for a few soils (e.g., Soil No. 3–14) can be due to a few outliers in the measured data in these soils. Fig. 6 provides a comparison between the measured and calibrated Poisson's ratio data values for Soil Nos. 1–18. The results show that the proposed PRCC can capture the measured data with good accuracy. For the plotted data in Fig. 6, the following statistical measure are obtained for a total of 221 data points: $R^2 = 0.93$, RMSE $= 0.02$, and RMSPE $= 15\%$.

Correlation with SWRC Parameters

Theoretically, as discussed previously, the PRCC is intrinsically related to the SWRC. Practically, it is useful to determine the fitting parameters of the proposed PRCC model in terms of well-known SWRC parameters, and these can be readily obtained from reported values in the literature or by running simple experimental tests. To statistically examine the relationship between the PRCC and SWRC, a linear regression analysis is performed between the PRCC parameters of S_{fun} and n_1 and the van Genuchten (1980) SWRC parameters of the residual degree of saturation (S_r) and pore size distribution (n). The linear regression analysis is performed using the data for five experimental data sets (Soil Nos. 19–23 in Table 1), where the SWRC data were available from the literature (Soil Nos. 19–22) or the current study (Soil No. 23).

Fig. 7(a) shows a linear correlation (with $R^2 = 0.99$ and P-value $= 2.37 \times 10^{-6}$) between the funicular degree of saturation and the residual degree of saturation. Similarly, Fig. 7(b) depicts a linear correlation (with $R^2 = 0.86$ and P-value $= 0.024$) between the pore size distribution and pore fluid connectivity parameters. The calculated P-value of smaller than 0.05 confirms the statistical significance of both correlations with 95% confidence. Using the correlations shown in Figs. 7(a and b), the following linear relationships are proposed:

$$S_{fun} = 1.04 S_r \tag{8}$$

$$n_1 = 0.27n + 2.57 \tag{9}$$

The presented correlations are incorporated into the proposed equation [Eq. (1)] to describe the PRCC in terms of the van Genuchten (1980) SWRC parameters as follows:

$$\mu = \mu_d + (\mu_s - \mu_d)\left[1 - \left\{1 + \left(\frac{S}{1.04S_r}\right)^{0.19n+2.71}\right\}^{1/(0.19n+2.71)-1}\right] \tag{10}$$

Using the van Genuchten (1980) SWRC model, one can also rewrite the PRCC model as a function of matric suction as

$$\mu = \mu_d + (\mu_s - \mu_d)\left[1 - \left\{1 + \left[\frac{S_r + (1-S_r)(1+(\alpha(u_a-u_w))^n)^{1/n-1}}{1.04S_r}\right]^{0.19n+2.71}\right\}^{1/(0.19n+2.71)-1}\right] \tag{11}$$

To examine the performance of Eq. (10), the SWRC parameters of n and S_r are collected for the five experimental data sets (Soil No. 19–23 in Table 1) and used to predict the PRCC of unsaturated soils. Fig. 8 shows the calibrated PRCC [using Eq. (1)] and the predicted PRCC using the SWRC parameters [using Eq. (10)] against the experimentally measured data sets for these five soils. The comparison demonstrates good agreement between the calibrated PRCC and SWRC-based PRCC predicted results against the measured values. Table 3 shows the statistical performance parameters calculated for the calibrated and predicted values

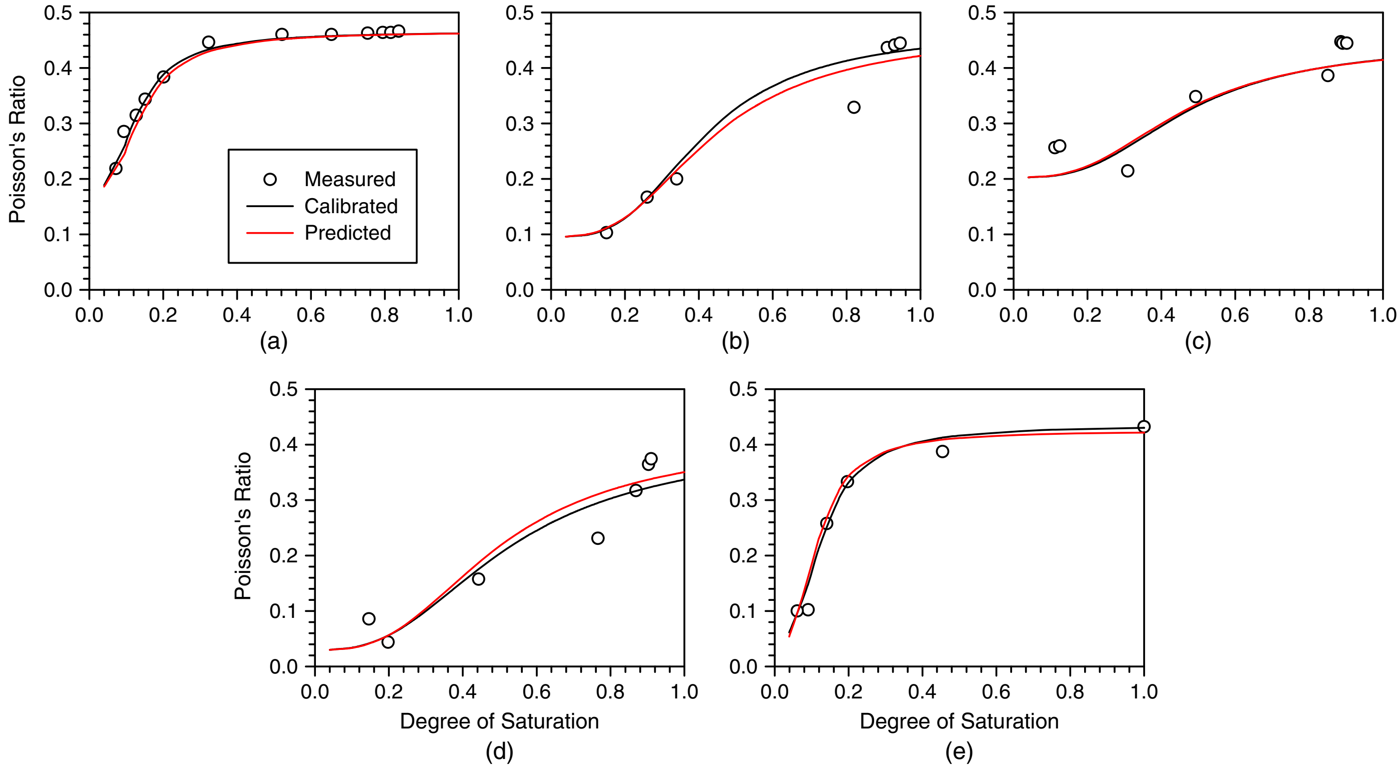

Fig. 8. Predicted and calibrated Poisson's ratio versus measured data for Soil Nos. 19–23.

for each soil. For both calibrated and predicted data, R^2 is greater than 0.90, the RMSE ranges between 0.01 and 0.04, and RMSPE ranges between 3% and 23% for all five soils. The low error demonstrates the good predictive accuracy of the proposed PRCC model with SWRC parameters. The overall results of the calibrated and predicted values indicate the fitting parameters of PRCC and SWRCs are well correlated. For all tested soils, the two curves differ by only a few percent with respect to the experimentally measured data. The difference could be attributed to the nonlinear variation of PRCC parameters with SWRC parameters. However, the error due to the assumption of linear correlation is practically negligible.

Application and Implication

To illustrate the implication of changes in Poisson's ratio with the degree of saturation, the coefficient of at-rest earth pressure in unsaturated soils is calculated using the proposed PRCC model as well as three constant Poisson's ratios of 0.1 (a very low Poisson's ratio representing highly compressible soils), 0.3 (a mid-range value for Poisson's ratio, which is very commonly used in analyses and simulations), and 0.45 (a very high Poisson's ratio representing relatively incompressible soils). The predicted results in terms of the coefficient of at-rest earth pressure are compared against the laboratory-measured data from the literature. One set of data is

Table 3. Statistical performance parameters of the proposed PRCC model calibrated using the experimental data and predicted using the SWRC data

	R^2		RMSE		RMSPE (%)	
Soil No.	Calibrated	Predicted	Calibrated	Predicted	Calibrated	Predicted
19	0.99	0.92	0.009	0.01	5.0	11.0
20	0.97	0.90	0.04	0.04	15.0	17.0
21	0.90	0.89	0.03	0.04	4.0	6.0
22	0.98	0.94	0.03	0.03	8.0	3.0
23	0.98	0.97	0.02	0.02	15.0	23.0

Table 4. Input parameters for at-rest earth pressure calculations

Soil	SWRC parameters	PRCC parameters
Silty sand[a]	$n = 1.55$, $\alpha = 0.06\ \mathrm{kPa}^{-1}$	$\mu_s = 0.46$, $\mu_d = 0.17$, $S_{fun} = 0.13$, $n_1 = 6.3$
Clay[b]	$n = 1.67$, $\alpha = 0.04\ \mathrm{kPa}^{-1}$	$\mu_s = 0.42$, $\mu_d = 0.08$, $S_{fun} = 0.12$, $n_1 = 2.9$
Sand and kaolin mixture[b]	$n = 1.66$, $\alpha = 0.06\ \mathrm{kPa}^{-1}$	$\mu_s = 0.395$, $\mu_d = 0.18$, $S_{fun} = 0.2$, $n_1 = 5$

[a]Measured data from Zhang et al. (2016).
[b]Measured data from Pirjalili et al. (2020).

J. Geotech. Geoenviron. Eng., 2021, 147(1): 04020149

obtained from Zhang et al. (2016) reporting results from suction-controlled oedometer tests conducted on silty sand. Further, two sets of laboratory-measured data are collected from Pirjalili et al. (2020), and they used a suction-controlled ring device to measure the coefficients of at-rest earth pressure for two soils (clay and sand + kaolin mixture) at various matric suctions (10–90 kPa).

For unsaturated soils, the coefficient of at-rest earth pressure can be defined as (Lu and Likos 2004):

$$K_0 = \frac{\mu}{1-\mu} - \frac{1-2\mu}{(1-\mu)(\sigma_v - u_a)}\chi(u_a - u_w) \tag{12}$$

where K_0 = coefficient of at-rest earth pressure for unsaturated soils; σ_v = normal stress, which can also be termed as the overburden pressure; and χ = Bishop's (1959) effective stress parameter, which can be represented by the effective degree of saturation, S_e (e.g., Lu and Likos 2004)

$$\chi = S_e = \frac{1}{(1+[\alpha(u_a-u_w)]^n)^{1-1/n}} \tag{13}$$

Combining Eqs. (1), (12), and (13), and the input parameters shown in Table 4, one can determine the coefficient of at-rest earth pressure at various matric suctions.

Fig. 9(a) shows the comparison between the measured versus predicted coefficient of at-rest earth pressure for the silty sand data. Figs. 9(b and c) show similar results for clay and sand-kaolin. The measured K_0 values are taken at the following net normal stresses for each soil from the original reference: 500 kPa for silty sand [Fig. 9(a)], 400 kPa for clay [Fig. 9(b)], and 200 kPa for sand-kaolin [Fig. 9(c)]. As shown with the measured data in Fig. 9, K_0 changes as the matric suction varies. The extent of this change depends on the soil type. For example, the change is more significant for silty sand [Fig. 9(a)] than the two other soils. The overall results predicted from the PRCC model show a very good match with the measured data for all three soils compared to the predicted values assuming a constant Poisson's ratio. Employing the proposed PRCC model into the calculation allows for a more accurate prediction of K_0 throughout the range of the matric suction.

As demonstrated in Fig. 9, using a constant Poisson's ratio can lead to several times smaller or larger, respectively, K_0 values than the measured values. For instance, using a Poisson's ratio of 0.3 (which is very commonly used in the conventional practice) continuously leads to about a 50%–100% underestimation of K_0 for the tested soils over the range of suctions examined. This also results in a 50%–100% underestimation of the resultant lateral thrust under at-rest conditions, which is significant. This example demonstrates the need to account for the effect of the degree of saturation on Poisson's ratio. The same level of importance can also be demonstrated for several other applications. For instance, Oh and Vanapalli (2018) used a set of finite element simulations and showed that changes in Poisson's ratio can notably influence the settlement and bearing capacity behaviors of shallow foundations in unsaturated cohesive soils.

This study is the first attempt in the literature to conceptualize and present a model for the PRCC. The model is developed and calibrated under small strain conditions. Soil stiffness is known to vary with strain levels and can be effaced by other factors such as confining pressure, void ratio, hydraulic hysteresis, and temperature. Further studies are needed to possibly extend the proposed model beyond small strain conditions and to examine the effects of confining pressure, void ratio, hydraulic hysteresis, and temperature on the PRCC. The model can benefit from more laboratory tests to further examine the relationship between the fitting parameters of the PRCC and the SWRC.

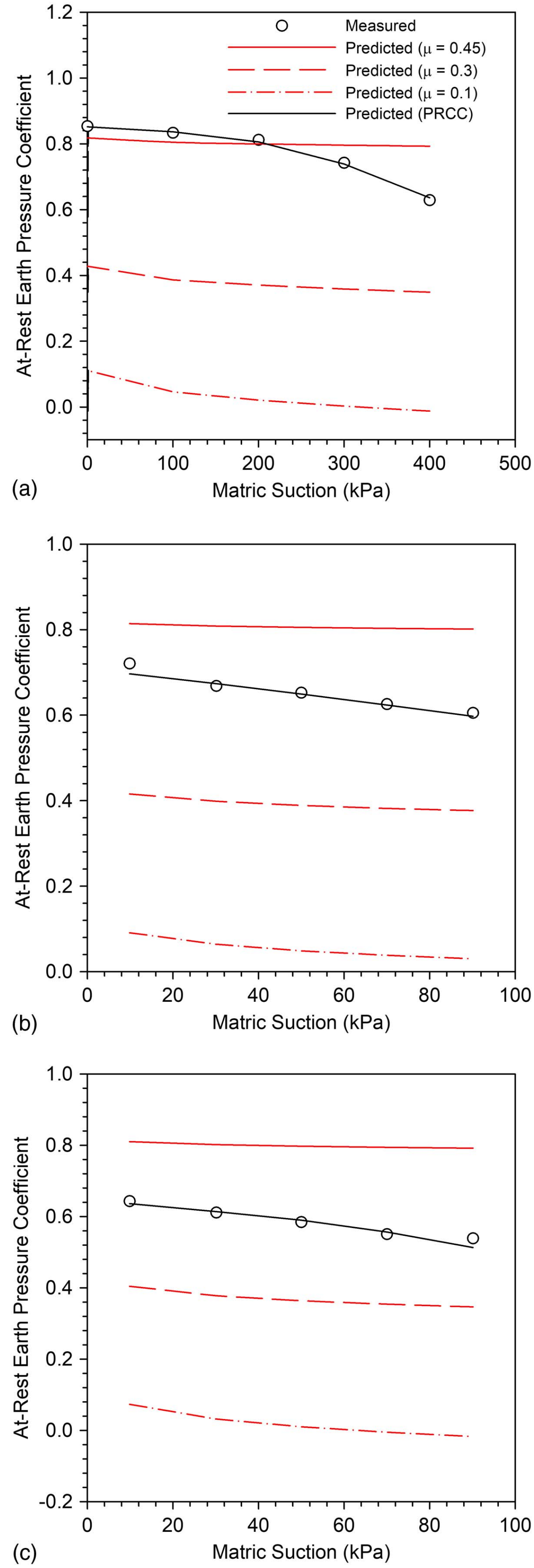

Fig. 9. At-rest earth pressure coefficient calculations using the PRCC model and constant Poisson's ratio values versus laboratory-measured data for (a) silty sand (measured data from Zhang et al. 2016); (b) clay; and (c) sand + kaolin mixture [measured data for (b and c) from Pirjalili et al. 2020].

J. Geotech. Geoenviron. Eng., 2021, 147(1): 04020149

Conclusions

Poisson's ratio is needed as input in the majority of geotechnical engineering applications involving stress-strain relationships. This study presented the concept of PRCC, capturing the evolution of Poisson's ratio due to variations in the degree of saturation (or matric suction) in unsaturated soils. The model was built based on the observation that the PRCC is dominated by water retention mechanisms and is intrinsically linked to the SWRC of unsaturated soils. A sigmoidal function is employed to mathematically describe the PRCC and calibrated and validated using experimental data sets of 23 different soils available in the literature as well as the tests performed in the current study. The proposed PRCC model requires two fitting parameters shown to linearly correlate to the SWRC fitting parameters to estimate Poisson's ratio of unsaturated soils at different degrees of saturation (or matric suctions). To demonstrate the implication of the PRCC model, the coefficient of at-rest earth pressure was evaluated with three constant Poisson's ratios values and the PRCC model. The comparison showed a very good match between the results from the PRCC model compared to the measured data. Further, the results demonstrated that ignoring the dependency of Poisson's ratio to the degree of saturation could lead to considerable errors in the calculated coefficient of at-rest earth pressure for unsaturated soils.

The proposed PRCC model provides a theoretically sound yet practical method to reasonably estimate Poisson's ratio of unsaturated soils. The model can readily be incorporated into analytical models and numerical simulations of unsaturated soils, leading to more accurate assessments of the behavior of unsaturated soils. The experimental test results demonstrated the dependence of Poisson's ratio on the water content in unsaturated soils. While the model can benefit from further validation against more experimental tests, the level of validation presented suffices to prove the validity of the proposed model.

Data Availability Statement

All data, models, and code generated or used during the study appear in the published article.

Acknowledgments

This material is based upon work supported in part by the National Science Foundation under Grant No. CMMI-1634748. Any opinions, findings, and conclusions or recommendations expressed in this material are those of the authors and do not necessarily reflect the views of the National Science Foundation.

References

Adamo, F., F. Attivissimo, L. Fabbiano, N. Giaquinto, and M. Spadavecchia. 2010. "Soil moisture assessment by means of compressional and shear wave velocities: Theoretical analysis and experimental setup." *Measurement* 43 (3): 344–352. https://doi.org/10.1016/j.measurement.2009.11.007.

Alramahi, B., K. A. Alshibli, and D. Fratta. 2010. "Effect of fine particle migration on the small-strain stiffness of unsaturated soils." *J. Geotech. Geoenviron. Eng.* 136 (4): 620–628. https://doi.org/10.1061/(ASCE)GT.1943-5606.0000244.

Alramahi, B., K. A. Alshibli, D. Fratta, and S. Trautwein. 2007. "A suction-control apparatus for the measurement of P and S-wave velocity in soils." *Geotech. Test. J.* 31 (1): 12–23. https://doi.org/10.1520/GTJ100646.

Ayres, A., and F. Theilen. 1999. "Relationship between P- and S-wave velocities and geological properties of near-surface sediments of the continental slope of the Barents Sea." *Geophys. Prospect.* 47 (4): 431–441. https://doi.org/10.1046/j.1365-2478.1999.00129.x.

Başer, T., Y. Dong, N. Lu, and J. S. McCartney. 2016. "Role of considering non-constant soil thermal parameters in the simulation of geothermal heat storage systems in the vadose zone." In *Proc., 8th Asian Young Geotechnical Engineers Conf.: Challenges and Innovations in Geotechnics*. Edited by A.Zhussupbekov, 137–142. Boca Raton, FL: CRC Press.

Bishop, A. W. 1959. "The principle of effective stress." *Teknisk Ukeblad* 106 (39): 859–863.

Budhu, M. 2010. *Soil mechanics and foundations*. 3rd ed. Hoboken, NJ: Wiley.

Byun, Y. H., J. S. Lee, S. H. Cho, and H. K. Yoon. 2013. "Evaluation of void ratio and elastic modulus of unsaturated soil using elastic waves." In *Proc., 18th Int. Conf. on Soil Mechanics and Geotechnical Engineering*, 1089–1092. London: International Society for Soil Mechanics and Geotechnical Engineering.

Cho, G. C., and J. C. Santamarina. 2001. "Unsaturated particulate materials—Particle-level studies." *J. Geotech. Geoenviron. Eng.* 127 (1): 84–96. https://doi.org/10.1061/(ASCE)1090-0241(2001)127:1(84).

Clayton, C. R. I. 2011. "Stiffness at small strain: Research and practice." *Géotechnique* 61 (1): 5–37. https://doi.org/10.1680/geot.2011.61.1.5.

Conte, E., R. M. Cosentini, and A. Troncone. 2009. "Geotechnical parameters from VP and VS measurements in unsaturated soils." *Soils Found.* 49 (5): 689–698. https://doi.org/10.3208/sandf.49.689.

Cosentini, R. M., and S. Foti. 2014. "Evaluation of porosity and degree of saturation from seismic and electrical data." *Géotechnique* 64 (4): 278. https://doi.org/10.1680/geot.13.P.075.

Dong, Y. 2019. "Dependency of poisson's ratio on water contents for unsaturated soils." Accessed August 23–25, 2019. https://www.jiban.or.jp/e/wp-content/uploads/2019/07/EA30_119apunsat2019.pdf.

Dong, Y., N. Lu, and J. S. McCartney. 2016. "A unified model for small-strain shear modulus of variably saturated soil." *J. Geotech. Geoenviron. Eng.* 142 (9): 04016039. https://doi.org/10.1061/(ASCE)GT.1943-5606.0001506.

Flammer, I., A. Blum, A. Leiser, and P. Germann. 2001. "Acoustic assessment of flow patterns in unsaturated soil." *J. Appl. Geophys.* 46 (2): 115–128. https://doi.org/10.1016/S0926-9851(01)00032-5.

Fredlund, D. G., H. Rahardjo, and M. D. Fredlund. 2012. *Unsaturated soil mechanics in engineering practice*. New York: Wiley.

Gao, W., C. W. Watts, T. Ren, H. C. Shin, S. Taherzadeh, K. Attenborough, and W. R. Whalley. 2013. "Estimating penetrometer resistance and matric potential from the velocities of shear and compression waves." *Soil Sci. Soc. Am. J.* 77 (3): 721–728. https://doi.org/10.2136/sssaj2012.0394.

Gupta, S. C., and W. E. Larson. 1979. "Estimating soil water retention characteristics from particle size distribution, organic matter percent, and bulk density." *Water Resour. Res.* 15 (6): 1633–1635. https://doi.org/10.1029/WR015i006p01633.

Inci, G., N. Yesiller, and T. Kagawa. 2003. "Experimental investigation of dynamic response of compacted clayey soils." *Geotech. Test. J.* 26 (2): 125–141. https://doi.org/10.1520/GTJ11328J.

Irfan, M., and T. Uchimura. 2013. "Effects of soil moisture on shear and dilatational wave velocities measured in laboratory triaxial tests." In *Proc., 5th Int. Young Geotechnical Engineering Conf.: Advances in Soil Mechanics and Geotechnical Engineerin*, 505–509. Amsterdam, Netherlands: IOS Press. https://doi.org/10.3233/978-1-61499-297-4-505.

Ishihara, K., Y. Huang, and H. Tsuchiya. 1998. "Liquefaction resistance of nearly saturated sand as correlated with longitudinal wave velocity." *Poromechanics—A tribute to Maurice*. Edited by A. Biot, J. F. Thimus, Y. Abousleiman, A. H. D. Cheng, O. Coussy, and E. Detournay. 583–586. Rotterdam, Netherlands: A.A. Balkema.

Kumar, J., and B. N. Madhusudhan. 2012. "Dynamic properties of sand from dry to fully saturated states." *Géotechnique* 62 (1): 45–54. https://doi.org/10.1680/geot.10.P.042.

Leong, E. C., and Z. Y. Cheng. 2016. "Effects of confining pressure and degree of saturation on wave velocities of soils." *Int. J. Geomech.*

16 (6): D4016013. https://doi.org/10.1061/(ASCE)GM.1943-5622.0000727.

Leverson, S. M., and R. A. Lohnes. 1995. "Moisture tension relations in sand." In *Proc., 1st Int. Conf. on Unsaturated Soils*, edited by E. E. Alonso and P. Delage, 387–392. Avereest, Netherlands: A.A. Balkema.

Likitlersuang, S., S. Teachavorasinskun, C. Surarak, E. Oh, and A. Balasubramaniam. 2013. "Small strain stiffness and stiffness degradation curve of Bangkok clays." *Soils Found.* 53 (4): 498–509. https://doi.org/10.1016/j.sandf.2013.06.003.

Lu, N., and Y. Dong. 2015. "Closed-form equation for thermal conductivity of unsaturated soils at room temperature" *J. Geotech. Geoenviron. Eng.* 141 (6): 04015016. https://doi.org/10.1061/(ASCE)GT.1943-5606.0001295.

Lu, N., and W. J. Likos. 2004. *Unsaturated soil mechanics*. New York: Wiley.

Lu, N., and W. J. Likos. 2006. "Suction stress characteristic curve for unsaturated soil." *J. Geotech. Geoenviron. Eng.* 132 (2): 131–142. https://doi.org/10.1061/(ASCE)1090-0241(2006)132:2(131).

Luna, R., and H. Jadi. 2000. "Determination of dynamic soil properties using geophysical methods." In *Proc., 1st Int. Conf. on the application of geophysical and NDT methodologies to transportation facilities and infrastructure*, 1–15. Washington, DC: Transportation Research Board.

Oh, W. T., and S. K. Vanapalli. 2011. "Relationship between Poisson's ratio and soil suction for unsaturated soils." In *Proc., 5th Asia-Pacific Conf. on Unsaturated Soils*, 239–245. Bangkok, Thailand: Kasetsart Univ.

Oh, W. T., and S. K. Vanapalli. 2016. "Influence of Poisson's ratio on the stress vs. settlement behavior of shallow foundations in unsaturated fine-grained soils." *Soils Rocks* 39 (1): 71–79.

Oh, W. T., and S. K. Vanapalli. 2018. "Modeling the stress versus settlement behavior of shallow foundations in unsaturated cohesive soils extending the modified total stress approach." *Soils Found.* 58 (2): 382–397. https://doi.org/10.1016/j.sandf.2018.02.008.

Patel, A., R. Ingale, and K. B. Bhanarkar. 2018. "Effect of compaction states and the confining pressure on Poisson's ratio of stratified and non-stratified soils." *Arabian J. Sci. Eng.* 43 (4): 1983–1999. https://doi.org/10.1007/s13369-017-2846-y.

Pietsch, W. 1991. *Size enlargement by agglomeration*. New York: Wiley.

Pirjalili, A., A. A. Garakani, A. Golshani, and A. Mirzaii. 2020. "A suction-controlled ring device to measure the coefficient of lateral soil pressure in unsaturated soils." *Geotech. Test. J.* 44 (1). https://doi.org/10.1520/GTJ20190099.

Salager, S., M. S. El Youssoufi, and C. Saix. 2007. "Influence of temperature on the water retention curve of soils. Modelling and experiments." In *Experimental unsaturated soil mechanics*, 251–258. Berlin: Springer.

Salem, H. S. 2000. "Poisson's ratio and the porosity of surface soils and shallow sediments, determined from seismic compressional and shear wave velocities." *Géotechnique* 50 (4): 461–463. https://doi.org/10.1680/geot.2000.50.4.461.

Saxton, K. E., W. J. Rawls, J. S. Romberger, and R. I. Papendick. 1986. "Estimating generalized soil-water characteristics from texture." *Soil Sci. Soc. Am. J.* 50 (4): 1031. https://doi.org/10.2136/sssaj1986.03615995005000040039x.

Shin, H. C., W. R. Whalley, K. Attenborough, and S. Taherzadeh. 2016. "On the theory of Brutsaert about elastic wave speeds in unsaturated soils." *Soil Tillage Res.* 156 (Mar): 155–165. https://doi.org/10.1016/j.still.2015.10.006.

Suwal, L. P., and R. Kuwano. 2013. "Statically and dynamically measured Poisson's ratio of granular soils on triaxial laboratory specimens." *Geotech. Test. J.* 36 (4): 20120108. https://doi.org/10.1520/GTJ20120108.

Tamura, S., K. Tokimatsu, A. Abe, and M. Sato. 2002. "Effects of air bubbles on B-value and P-wave velocity of a partly saturated sand." *Soils Found.* 42 (1): 121–129. https://doi.org/10.3208/sandf.42.121.

Taylor, O. D. S., A. L. Cunningham, R. E. Walker, M. H. McKenna, K. E. Martin, and P. G. Kinnebrew. 2019. "The behavior of near-surface soils through ultrasonic near-surface inundation testing." *Near Surf. Geophys.* 17 (4): 331–344. https://doi.org/10.1002/nsg.12045.

Tsukamoto, Y., K. Ishihara, H. Nakazawa, K. Kamada, and Y. Huang. 2002. "Resistance of partly saturated sand to liquefaction with reference to longitudinal and shear wave velocities." *Soils Found.* 42 (6): 93–104. https://doi.org/10.3208/sandf.42.6_93.

Valle-Molina, C. 2006. "Measurements of Vp and Vs in dry, unsaturated and saturated sand specimens with piezoelectric transducers." Doctoral dissertation, Dept. of Civil, Architecture and Environmental Engineering, Univ. of Texas at Austin.

van Genuchten, M. T. 1980. "A closed-form equation for predicting the hydraulic conductivity of unsaturated soils." *Soil Sci. Soc. Am. J.* 44 (5): 892–898. https://doi.org/10.2136/sssaj1980.03615995004400050002x.

Velea, D., F. D. Shields, and J. M. Sabatier. 2000. "Elastic wave velocities in partially saturated Ottawa sand." *Soil Sci. Soc. Am. J.* 64 (4): 1226–1234. https://doi.org/10.2136/sssaj2000.6441226x.

Vereecken, H., J. Maes, J. Feyen, and P. Darius. 1989. "Estimating the soil moisture retention characteristic from texture, bulk density, and carbon content." *Soil Sci.* 148 (6): 389–403. https://doi.org/10.1097/00010694-198912000-00001.

Wang, J.-P., N. Hu, B. Francois, and P. Lambert. 2017. "Estimating water retention curves and strength properties of unsaturated sandy soils from basic soil gradation parameters." *Water Resour. Res.* 53 (7): 6069–6088. https://doi.org/10.1002/2017WR020411.

Yang, J., and X. Q. Gu. 2013. "Shear stiffness of granular material at small strains: Does it depend on grain size?" *Géotechnique* 63 (2): 165–179. https://doi.org/10.1680/geot.11.P.083.

Zhang, X., E. E. Alonso, and F. Casini. 2016. "Explicit formulation of at-rest coefficient and its role in calibrating elasto-plastic models for unsaturated soils." *Comput. Geotech.* 71 (Jan): 56–68. https://doi.org/10.1016/j.compgeo.2015.08.012.